Mon. Not. R. Astron. Soc. **389,** 1336–1344 (2008) doi:10.1111/j.1365-2966.2008.13644.x

Reddenings of FGK supergiants and classical Cepheids from spectroscopic data

V. V. Kovtyukh,[1⋆] C. Soubiran,[2] R. E. Luck,[3] D. G. Turner,[4] S. I. Belik,[1] S. M. Andrievsky[1,5] and F. A. Chekhonadskikh[5]

[1]*Astronomical Observatory, Odessa National University, T. G. Shevchenko Park, 65014 Odessa, Ukraine*
[2]*Université de Bordeaux – CNRS – Laboratoire d'Astrophysique de Bordeaux, BP 89, 33270 Floirac, France*
[3]*Department of Astronomy, Case Western Reserve University, 10900 Euclid Avenue, Cleveland, OH 44106-7215, USA*
[4]*Department of Astronomy and Physics, Saint Mary's University, Halifax, Nova Scotia, Canada B3H 3C3*
[5]*Department of Astronomy, Odessa National University, T. G. Shevchenko Park, 65014 Odessa, Ukraine*

Accepted 2008 June 25. Received 2008 June 25; in original form 2008 May 30

ABSTRACT

Accurate and homogeneous atmospheric parameters ($T_{\rm eff}$, $\log g$, $V_{\rm t}$, [Fe/H]) are derived for 74 FGK non-variable supergiants from high-resolution, high signal-to-noise ratio, echelle spectra. Extremely high precision for the inferred effective temperatures (10–40 K) is achieved by using the line-depth ratio method. The new data are combined with atmospheric values for 164 classical Cepheids, observed at 675 different pulsation phases, taken from our previously published studies. The derived values are correlated with unreddened $B - V$ colours compiled from the literature for the investigated stars in order to obtain an empirical relationship of the form $(B - V)_0 = 57.984 - 10.3587(\log T_{\rm eff})^2 + 1.675\,72(\log T_{\rm eff})^3 - 3.356 \log g + 0.0321 V_{\rm t} + 0.2615[{\rm Fe/H}] + 0.8833(\log g)(\log T_{\rm eff})$. The expression is used to estimate colour excesses $E(B - V)$ for individual supergiants and classical Cepheids, with a precision of ± 0.05 mag for supergiants and Cepheids with $n = 1$–2 spectra, reaching ± 0.025 mag for Cepheids with $n > 2$ spectra, matching uncertainties for the most sophisticated photometric techniques. The reddening scale is also a close match to the system of space reddenings for Cepheids. The application range is for spectral types F0–K0 and luminosity classes I and II.

Key words: stars: fundamental parameters – supergiants – Cepheids.

1 INTRODUCTION

The Cepheid period–luminosity (PL) relation continues to play a key role in the determination of distances within the Local Group and to nearby galaxies. The absolute calibration of the PL relation requires reliable distance measurements for calibrating Cepheids as well as accurate corrections for the effects of interstellar reddening and extinction. Galactic Cepheids are often heavily obscured, the average colour excess $E(B - V)$ being of the order of 0.5 mag. Here we propose a new method of accurate colour excess determination that relies on spectroscopically determined stellar parameters.

The traditional methods of establishing the interstellar reddening of Cepheids have involved field reddenings derived from photometric and spectroscopic studies of stars surrounding the Cepheid, the use of reddening-independent spectroscopic indices, and period–colour relations calibrated from spectroscopic analyses of a number of well-studied Cepheids or supergiants. Field reddenings are fairly reliable provided that the surrounding stars are unaffected by circumstellar reddening, although the number of suitable objects has tended to be restricted to cluster Cepheids and visual binaries (see Turner 1995, 2001; Laney & Caldwell 2007). Reddening-independent indices include the Γ index (Kraft 1960; Spencer Jones 1989), which measures the depression in stellar spectra caused by the *G* band of CH (λ4305), and the *KHG* index (McNamara & Potter 1969; McNamara, Helm & Wilcken 1970; Feltz 1972; Turner, Leonard & English 1987), which combines narrow-band photometry of Ca II K (λ3933), Balmer Hδ (λ4101) and the *G* band. Narrow-band photometry of Balmer Hβ (λ4861) has also been used as a temperature indicator for FGK stars, but has been susceptible to problems arising from colour dependences introduced by mismatches in the effective wavelengths of the narrow and wide Hβ filters employed (Schmidt & Taylor 1979).

Most Cepheid reddenings have been derived from period–colour relations that are tied to specific Cepheid or supergiant calibrators, in which specific continuum or spectral line features (line ratios, for example) are linked to stellar atmosphere models to infer effective temperatures for the stars (e.g. Fernie 1987; Sasselov & Lester 1990). The direct link between effective temperature and broad-band $(B - V)_0$ colour has been demonstrated very effectively by

⋆E-mail: val@deneb1.odessa.ua

Gray (1992) for older, published, stellar atmosphere models, and has been used successfully to test the open cluster calibration of the PL relation (Turner & Burke 2002). As argued by Fry & Carney (1999), $B - V$ colours for Cepheids appear to be more closely indicative of stellar temperatures than indices that include a near-infrared magnitude. But recent changes to stellar atmosphere models (Kurucz 1992) may affect the effective temperature scale for FGK supergiants significantly enough that a recalibration is necessary. That is the purpose of the present paper.

Cepheids also undergo significant changes in effective temperature during their pulsation cycles, which makes it essential to track such changes accurately through close monitoring of individual variables. Photometric monitoring of Cepheids has resulted in a large data base of published results for many different colour systems (Berdnikov 2007), but the availability of high-resolution spectra for such stars throughout their cycles has been extremely limited, until now. A goal of the present paper is therefore to exploit a recently developed collection of high-resolution spectra for Galactic Cepheids in order to present accurate intrinsic parameters for all of the studied objects.

2 OBSERVATIONS

The spectra of the FGK supergiants studied here were obtained using the 1.93-m telescope of the Haute-Provence Observatoire (France) equipped with the echelle spectrograph ELODIE (Baranne et al. 1996) and retrieved from its online archive of spectra (Moultaka et al. 2004). The resolving power for the observations was $R = 42\,000$ over the wavelength interval 4400–6800 Å, with a signal-to-noise ratio for each spectrum of S/N $\geq$ 100 (at 5500 Å). Initial processing of the spectra (image extraction, cosmic ray removal, flat-fielding, etc.) was carried out as described by Katz et al. (1998).

We also made use of spectra obtained with the Ultraviolet–Visual Echelle Spectrograph (UVES) instrument at the Very Large Telescope (VLT) Unit 2 Kueyen (Bagnulo et al. 2003). All supergiants were observed in two instrumental modes, Dichroic 1 (DIC1) and Dichroic 2 (DIC2), in order to provide almost complete coverage of the wavelength interval 3000–10 000 Å. The spectral resolution is about 80 000, and for most of the spectra the typical S/N is 300–500 in the V band.

For classical Cepheids in our sample we have used our previously published results (Kovtyukh & Andrievsky 1999; Andrievsky et al. 2002a,b,c; Luck et al. 2003; Andrievsky, Luck & Kovtyukh 2005; Kovtyukh et al. 2005; Luck, Kovtyukh & Andrievsky 2006). Multiphase observations of programme Cepheids were carried out using the Struve 2.1-m reflector and Sandiford echelle spectrograph at McDonald Observatory. The nominal resolving power was 60 000 with a total spectral range covering about 1000–1200 Å. The primary wavelength region was centred at 6200 Å. Exposure times were selected to ensure an optimal S/N of about 100.

Additional processing of the spectra (continuum level location, measuring of line depths and equivalent widths) was carried out using the DECH20 software (Galazutdinov 1992). Line depths R_λ were measured by means of Gaussian fitting.

3 ATMOSPHERIC PARAMETERS FOR FGK SUPERGIANTS AND CLASSICAL CEPHEIDS

Effective temperatures for our programme stars were established from the processed spectra using the method developed by Kovtyukh (2007) that is based upon $T_{\rm eff}$–line depth relations. The technique can establish $T_{\rm eff}$ with exceptional precision. It relies upon the ratio of the central depths of two lines that have very different functional dependences on $T_{\rm eff}$, and uses tens of pairs of lines for each spectrum. The method is independent of interstellar reddening, and only marginally dependent on the individual characteristics of stars, such as rotation, microturbulence, metallicity, etc.

Briefly, a set of 131 line ratio–$T_{\rm eff}$ relations was employed, with the mean random error in a single calibration being 60–90 K (40–45 K in most cases and 90–95 K in the least accurate cases). The use of ~70–100 calibrations per spectrum reduces the uncertainty in $T_{\rm eff}$ to 10–20 K for spectra with S/N values greater than 100, and 30–50 K for spectra with S/N values less than 100. Although the internal error for each $T_{\rm eff}$ determination appears to be small, a systematic shift of the zero-point in the $T_{\rm eff}$ scale may exist. Nevertheless, an uncertainty in zero-point (if it exists) can affect the absolute abundances derived for each programme star. It is relatively unimportant for abundance comparisons between stars in the sample. For the majority of supergiants and Cepheids we obtain error estimates for $T_{\rm eff}$ that are smaller than 10–40 K.

The microturbulent velocities, $V_{\rm t}$, and surface gravities, $\log g$, were derived using a modification of the standard analysis proposed by Kovtyukh & Andrievsky (1999). As described there, the microturbulence is determined from the Fe II lines rather than the Fe I lines, as in classical abundance analyses. The surface gravity is established by forcing equality between the total iron abundance obtained from both Fe I and Fe II lines. Typically with this method the iron abundance determined from Fe I lines shows a strong dependence on equivalent width (NLTE effects), so we take as the proper iron abundance the extrapolated total iron abundance at zero equivalent width.

Kurucz's WIDTH9 code was used with an atmospheric model for each star interpolated from a grid of models calculated with a microturbulent velocity of 4 km s^{-1}. At some phases Cepheids can have microturbulent velocities deviating significantly from that value; however, our previous test calculations suggest that changes in the model microturbulence over a range of several km s^{-1} has an insignificant impact on the resulting element abundances. Typical results obtained for the Cepheid δ Cep over its cycle are shown for illustrative purposes in Fig. 1.

Final results for our determinations of $T_{\rm eff}$, $\log g$, $V_{\rm t}$ (in km s^{-1}) and [Fe/H] for FGK supergiants in our sample are given in Table 1. Typical uncertainties in the cited values are $\pm$(10–40) K in $T_{\rm eff}$, $\pm$0.1 in $\log g$ and $\pm$0.5 km s^{-1} in $V_{\rm t}$.

4 COLOUR EXCESSES

Values of $T_{\rm eff}$, $\log g$, $V_{\rm t}$ and [Fe/H] obtained in the described manner can be used to determine intrinsic colours for the target Cepheids and FGK supergiants in our sample. As noted earlier, the effective temperature $T_{\rm eff}$ of an FGK supergiant can be linked to intrinsic $(B - V)_0$ colour using relationships such as that of Gray (1992). For this paper, however, a recalibration was made using unreddened $(B - V)_0$ colours from Bersier (1996) for supergiants and from Fernie et al. (1995), Tammann, Sandage & Reindl (2003) and Laney & Caldwell (2007) for Cepheids. Any disadvantages arising from combining different sources of reddening for the Cepheids appear to be negligible, as discussed in the following section. For Cepheids in the sample, an instantaneous 'observed' $B - V$ colour index was obtained from the extensive data base of Berdnikov (2007), which contains multicolour photoelectric observations for all of our 164 programme Cepheids. Published ephemerides were used to

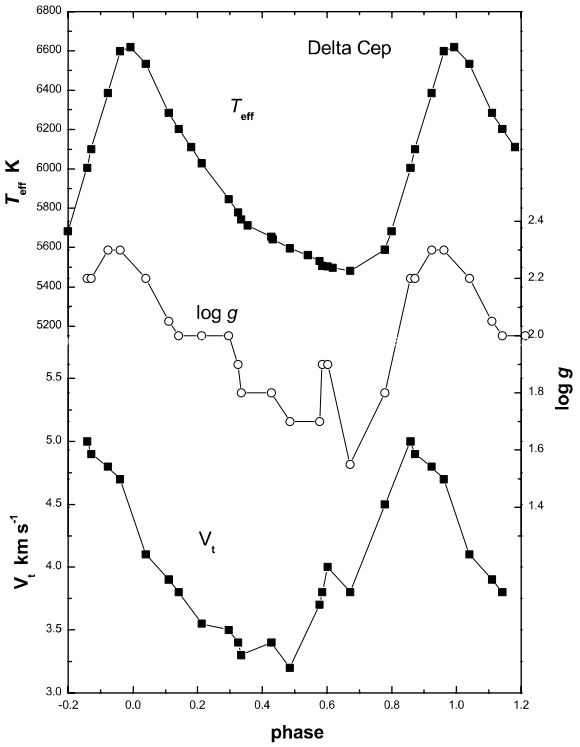

Figure 1. The variation of $T_{\rm eff}$, $\log g$ and $V_{\rm t}$ for δ Cep.

phase the data, and the light curves were subjected to Fourier analysis, with coefficients determined up to the third to tenth order, in order to match them (see Figs 2 and 3).

Published ephemerides were also used to derive pulsation phases for the times of the individual spectroscopic observations. In such fashion a pair of reddened and unreddened $B - V$ values was generated for each epoch of spectroscopic observation for a Cepheid. Since the colour excess should not vary during a pulsation cycle, multivariate least squares can be used to link the observed intrinsic parameters for Cepheids and supergiants to intrinsic $(B - V)_0$ colour.

Problems can arise when comparing photometric and spectroscopic data from different epochs, particularly for long-period Cepheids which undergo very rapid changes in pulsation period relative to Cepheids of short period (see Turner, Abdel-Sabour Abdel-Latif & Berdnikov 2006a). To minimize such problems, modern elements (quadratic, for example) from Berdnikov (2007) were used to tie phases of spectroscopic observation to those for nearby (close) epochs of photometric observation. But it was not always possible to minimize the differences between epochs of photometric and spectroscopic observation for all Cepheids, with Southern hemisphere objects remaining as a potential source of error.

In summary, the method takes known atmospheric parameters ($T_{\rm eff}$, $\log g$, $V_{\rm t}$, [Fe/H]) for the supergiants and Cepheids, and adopts a colour excess $E(B - V)$ from Bersier (1996), Fernie et al. (1995), Tammann et al. (2003) and Laney & Caldwell (2007). For objects common to those studies, the values were averaged. An observed value of $B - V$ for the supergiant or Cepheid was obtained next, in the case of Cepheids using data from Berdnikov (2007) phased in the same manner as the spectroscopic data, as noted above. The analysis therefore yields $(B - V)_0$ for the supergiants, and comparable values for the Cepheids at the observed phases. A multivariate regression of ($T_{\rm eff}$, $\log g$, $V_{\rm t}$, [Fe/H]) versus $(B - V)_0$ was then performed on the 693 individual observations to produce the following relationship: $(B - V)_0 = (57.984 \pm 4.485) - (10.3587 \pm 0.9797)(\log T_{\rm eff})^2 + (1.675\,72 \pm 0.176\,31)(\log T_{\rm eff})^3 - (3.356 \pm 0.461)\log g + (0.0321 \pm 0.0024)V_{\rm t} + (0.2615 \pm 0.0301)$[Fe/H] $+ (0.8833 \pm 0.1229)(\log g)(\log T_{\rm eff})$.

With the above relationship it was possible to derive homogeneous colour excesses $E(B - V) = (B - V) - (B - V)_0$ for 74 FGK supergiants and 164 classical Cepheids. The former are presented in Table 1, the latter are summarized in Table 2. The precision in the final estimates of $(B - V)_0$ is estimated to be 0.04–0.05 mag (1σ, external precision) for spectra of $R = 42\,000$, S/N = 100–150. The internal precision is 0.0025 mag. The results could be improved further with the addition of higher resolution and larger S/N spectra. We note that the error budget does not include possible uncertainties that arise from the individual properties of stars, such as rotation, chemical composition, binarity, etc.

5 RESULTS

Tables 1 and 2 list the results for FGK supergiants and classical Cepheids, respectively. For Cepheids the variable star designation and pulsation period P are listed in columns (1) and (2), respectively, the mean colour excess determined here is listed in column (3), the standard error of the mean is listed in column (4), and the number of determinations used to calculate the mean is listed in column (5). The mean value of $E(B - V)$ was obtained by averaging the values of $E(B - V)$ over the pulsation cycle. Individual reddenings estimated by Fernie et al. (1995), Tammann et al. (2003) and Laney & Caldwell (2007) are also listed for convenience in Table 2, in columns (5), (6) and (7), respectively. A comparison of the reddenings of Fernie et al. (1995) with the present results is shown in Fig. 4, and comparisons with the reddenings of Tammann et al. (2003) and Laney & Caldwell (2007) are shown in Figs 5 and 6.

A statistical comparison of the present Cepheid reddenings was made with an overlapping set of space reddenings for 27 stars in common. The space reddenings are those summarized by Laney & Caldwell (2007), but with additional data used in a previous analysis of Cepheid reddenings (Turner 2001) that includes new estimates for previously unstudied objects (Turner et al. 2008). Four of the objects in the sample display large differences in reddening between the two data sets, in excess of $\Delta E(B - V) = 0.1$, namely V Cen, S Nor, VY Sgr and WZ Sgr. All are Southern hemisphere Cepheids, noted to be a problem in the previous section, and the first three have only single spectroscopic observations available. Multiple observations ($n = 12$) exist for WZ Sgr, but its space reddening has been noted previously to be a problem (Laney & Caldwell 2007). For the 23 remaining Cepheids the difference in colour excesses $\Delta E(B - V)$ (space reddening – spectroscopic reddening) is $+0.005 \pm 0.039$ s.d., and $+0.000 \pm 0.035$ s.d. for the 16 Cepheids with multiple spectroscopic observations. It appears that the present compilation of spectroscopic reddenings for Cepheids is tied closely to the system of available space reddenings. In addition, since the average uncertainty for the space reddenings of individual Cepheids in the sample is ± 0.024, the precision of the spectroscopic reddenings based upon multiple spectra must be ± 0.025, while the accuracy matches that of the space reddening system.

The reddening system of the present paper also appears to be closely matched to older reddening systems for Cepheids, as indicated by the trends of Figs 4–6. The scatter in the plots of Figs 4 and 5 is suggestive of actual differences that may exist, which may have several explanations. Period–colour relations, for example, do not always account for the intrinsic dispersion of

Table 1. Computed colour excesses for FGK supergiants. Negative $E(B-V)$ values are set to zero.

HD	$T_{\rm eff}$	log g	$V_{\rm t}$	[Fe/H]	$E(B-V)$	HD/BD	$T_{\rm eff}$	log g	$V_{\rm t}$	[Fe/H]	$E(B-V)$
000725	7053	2.1	6.3	−0.04	0.271	171635	6151	2.15	5.2	−0.04	0.051
001457	7636	2.3	4.8	−0.04	0.394	172365	6196	2.5	7.5	−0.07	0.180
004362	5301	1.6	4.4	−0.15	0.219	173638	7444	2.4	4.7	0.11	0.302
007927	7341	1.0	8.7	−0.24	0.425	174104	5657	3.1	4.8	−0.02	0.045
008890	6008	2.2	4.35	0.07	−0.007	179784	4956	2.0	2.5	0.08	0.394
008906	6710	2.2	4.8	−0.07	0.350	180028	6307	1.9	4.0	0.10	0.320
009900	4529	1.7:	2.7	0.10	0.073	182296	5072	2.1	3.6	0.17	0.321
009973	6654	2.0	5.7	−0.05	0.434	182835	6969	1.6	4.9	0.00	0.268
010494	6672	1.25	7.5	−0.20	0.813	183864	5323	1.8	3.5	−0.02	0.425
011544	5126	1.4	3.5	0.01	0.174	185758	5367	2.4	2.1	−0.03	0.037
016901	5505	1.7	4.3	−0.03	0.110	187203	5710	2.2	5.1	0.05	0.222
017971	6822	1.3	8.7	−0.20	0.644	187299	4566	1.2	3.5	0.03	0.257
018391	5756	1.2	11.5	0.02	0.991	187428	5892	2.4:	2.9	0.02	0.177
020902	6541	2.0	4.8	−0.01	0.039	190113	4784	1.9	3.5	0.05	0.360
025056	5752	2.1	5.6	0.15	0.437	190403	4894	2.0	2.5	0.09	0.133
025291	7497	2.65	4.1	0.00	0.241	191010	5253	2.1:	1.9	0.05	0.171
026630	5309	1.8	3.7	0.02	0.085	194093	6244	1.7	6.1	0.05	0.087
032655	6755	2.7	5.0	−0.12	0.059	195295	6572	2.4	3.5	0.01	0.001
032655	6653	2.5	5.0	−0.13	0.044	200102	5364	1.6	3.3	−0.13	0.250
036673	7500	2.3	4.4	0.07	−0.046	200805	6865	2.2	4.6	−0.03	0.455
036891	5089	1.7	3.3	−0.06	0.081	202314	5004	2.1	3.2	0.12	0.082
039949	5239	2.0:	3.3	−0.05	0.233	202618	6541	2.8	4.0	−0.16	0.053
044391	4599	1.6	3.4	0.03	0.119	204022	5337	1.5:	3.9	0.01	0.602
045348	7557	2.2	2.7	−0.10	0.016	204075	5262	2.0	2.6	−0.08	0.186
047731	4989	2.0	3.2	0.02	0.092	204867	5431	1.6	4.15	−0.04	0.006
048329	4583	1.2	3.7	0.16	0.021	206859	4912	1.2	2.5	0.04	0.065
052497	5090	2.45	3.6	−0.02	0.033	207489	6350	2.85	5.6	0.13	0.119
054605	6364	1.5	10.2	−0.03	0.085	208606	4702	1.4	4.0	0.11	0.323
057146	5126	1.9	3.6	0.17	−0.019	209750	5199	1.4	3.55	0.02	0.022
061227	7433	2.5	5.5	−0.16	0.284	210848	6238	3.0	3.2	0.08	0.001
074395	5247	1.8	3.0	−0.01	−0.028	216206	5003	2.1	3.2	0.02	0.158
077912	4975	2.0	2.4	0.01	0.061	218600	7458	2.4:	4.8	−0.07	0.653
084441	5281	2.15	2.15	−0.01	0.006	219135	5430	1.75	3.6	−0.01	0.296
092125	5336	2.4	2.7	0.05	0.020	220102	6832	2.5	5.8	−0.23	0.262
159181	5214	2.2	3.4	0.04	0.087	223047	4864	1.7	3.4	0.07	−0.005
164136	6483	3.1	4.5	−0.37	0.018	224165	4804	1.9	2.5	0.08	0.064
171237	6792	2.6	4.4	−0.09	0.175	+60 2532	6268	1.8	5.2	−0.01	0.597

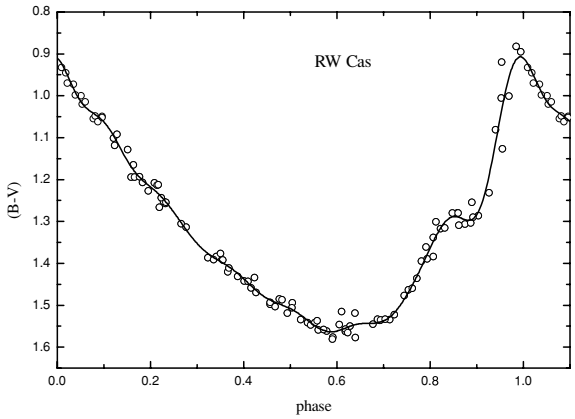

Figure 2. $B-V$ colour curve for RW Cas. The Fourier fit is shown as a line.

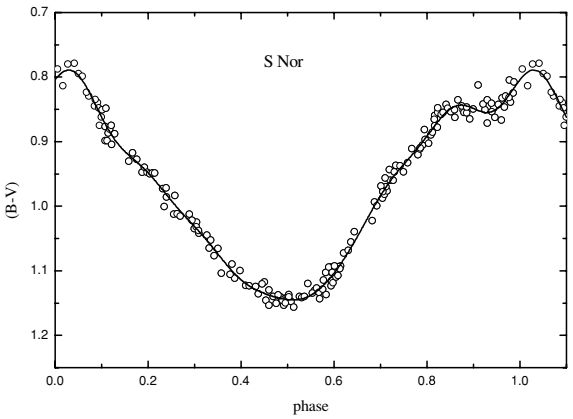

Figure 3. As in Fig. 2 but for S Nor.

Cepheids within the instability strip. Small amplitude Cepheids tend to lie on the hot edge of the strip, for example (Pel & Lub 1978; Turner et al. 2006a), so their reddenings can be underestimated by period–colour relations. Large amplitude Cepheids lie near the centre of the strip (e.g. Turner et al. 2006a), but may not always be representative of the calibrators used. Although similar scatter is seen in Fig. 6, where the present results are compared with the space reddening system of Laney & Caldwell (2007), the

Table 2. Computed colour excesses for classical Cepheids.

Name	P (d)	$E(B-V)$	±	No. of spectra	$E(B-V)_{\rm Fer95}$	$E(B-V)_{\rm TSR03}$	$E(B-V)_{\rm LC07}$
U Aql	7.023 958	0.416	–	1	0.401	0.371	0.364
SZ Aql	17.140 849	0.588	0.041	11	0.588	0.552	0.531
TT Aql	13.754 707	0.480	0.036	8	0.518	0.462	0.432
FF Aql	4.470 916	0.224	0.017	14	0.208	–	0.191
FM Aql	6.114 230	0.636	0.010	3	0.676	0.617	0.595
FN Aql	9.481 603	0.469	0.016	5	0.517	0.490	0.488
V496 Aql	6.807 055	0.408	0.009	3	0.453	–	0.390
V600 Aql	7.238 748	0.830	–	1	0.864	0.819	0.792
V733 Aql	6.178 748	0.106	–	1	–	–	–
V1162 Aql	5.376 100	0.163	–	1	0.196	0.187	–
V1344 Aql	7.478 030	0.544	–	2	0.626	0.569	–
Eta Aql	7.176 735	0.096	0.015	14	0.152	0.133	0.138
V340 Ara	20.809 000	0.540	–	1	0.583	0.546	–
RT Aur	3.728 190	0.050	0.036	10	0.063	0.049	0.089
SY Aur	10.144 698	0.457	–	1	0.411	0.453	–
YZ Aur	18.193 212	0.580	0.030	5	0.583	0.601	0.575
AN Aur	10.290 560	0.559	0.051	3	0.577	0.600	–
BK Aur	8.002 432	0.396	–	1	0.418	0.424	–
CY Aur	13.847 650	0.905	–	1	0.837	0.767	–
ER Aur	15.690 730	0.618	–	1	0.491	0.494	–
V335 Aur	3.413 250	0.701	–	1	0.658	0.626	–
RY CMa	4.678 250	0.232	–	1	0.253	0.223	0.258
TW CMa	6.995 070	0.311	–	1	0.398	0.391	0.280
VZ CMa	3.126 230	0.537	–	1	0.474	–	–
RX Cam	7.912 024	0.539	0.034	9	0.581	0.536	0.553
TV Cam	5.294 970	0.482	–	1	0.596	0.612	–
AB Cam	5.787 640	0.681	–	1	0.662	0.673	–
AD Cam	11.260 991	0.939	–	1	0.929	0.871	–
RW Cas	14.791 548	0.415	–	2	0.468	0.409	0.383
RY Cas	12.138 880	0.580	–	1	0.676	0.613	–
SU Cas	1.949 322	0.296	0.026	13	0.288	–	0.282
SW Cas	5.440 950	0.517	–	1	0.505	0.449	0.484
SY Cas	4.071 098	0.449	–	1	0.478	0.430	–
SZ Cas	13.637 747	0.949	–	1	0.759	–	0.809
XY Cas	4.501 697	0.494	–	1	0.550	0.480	–
BD Cas	3.650 900	1.006	–	1	–	–	–
CEa Cas	5.141 058	0.503	–	1	0.591	0.562	–
CEb Cas	4.479 301	0.479	–	1	0.576	0.548	–
CF Cas	4.875 220	0.527	0.025	5	0.591	0.531	0.544
CH Cas	15.086 190	0.907	–	1	1.002	0.955	–
CY Cas	14.376 860	0.891	–	1	1.013	0.947	–
DD Cas	9.812 027	0.439	–	1	0.517	0.493	0.446
DL Cas	8.000 669	0.487	0.024	14	0.518	0.479	0.499
FM Cas	5.809 284	0.324	–	1	0.350	0.290	0.309
V379 Cas	4.305 750	0.600	–	1	–	–	–
V636 Cas	8.377 000	0.553	0.012	8	0.631	–	–
V Cen	5.493 861	0.167	–	1	0.282	0.264	0.311
CP Cep	17.859 000	0.659	–	1	0.724	0.702	–
CR Cep	6.232 964	0.721	–	1	0.749	0.697	0.698
IR Cep	2.114 124	0.368	–	1	0.434	–	–
V351 Cep	2.805 910	0.436	–	1	–	–	–
Delta Cep	5.366 270	0.045	0.018	18	0.080	0.068	0.087
BG Cru	3.342 720	0.087	–	1	0.111	–	–
X Cyg	16.386 332	0.239	0.029	26	0.267	0.261	0.208
SU Cyg	3.845 492	0.074	0.019	12	0.133	0.088	0.091
SZ Cyg	15.109 642	0.576	–	1	0.632	0.587	0.562
TX Cyg	14.708 157	1.112	–	1	1.195	1.111	1.179
VX Cyg	20.133 407	0.830	–	1	0.889	0.830	–
VY Cyg	7.856 982	0.639	–	1	0.634	0.615	0.597
VZ Cyg	4.864 453	0.246	–	1	0.310	0.274	0.270
BZ Cyg	10.141 932	0.872	–	1	0.885	0.839	–

Table 2 – *continued*

Name	P (d)	$E(B-V)$	±	No. of spectra	$E(B-V)_{\rm Fer95}$	$E(B-V)_{\rm TSR03}$	$E(B-V)_{\rm LC07}$
CD Cyg	17.073 967	0.447	0.040	16	0.545	0.486	0.513
DT Cyg	2.499 082	0.028	0.009	14	0.067	–	0.048
MW Cyg	5.954 586	0.692	–	1	0.693	0.615	0.645
V386 Cyg	5.257 606	0.891	–	1	0.965	0.884	0.844
V402 Cyg	4.364 836	0.366	–	1	0.484	0.397	0.391
V532 Cyg	3.283 612	0.568	–	1	0.552	–	0.453
V924 Cyg	5.571 472	0.233	–	1	0.258	–	0.256
V1154 Cyg	4.925 460	0.234	–	1	0.335	–	–
V1334 Cyg	3.333 020	0.025	0.009	11	−0.055	–	–
V1726 Cyg	4.237 060	0.318	–	1	0.312	–	0.361
TX Del	6.165 907	0.222	–	1		–	–
Beta Dor	9.842 425	0.000	–	1	0.080	0.069	0.041
W Gem	7.913 779	0.273	0.040	11	0.281	0.266	0.252
AA Gem	11.302 328	0.231	–	1	0.367	0.380	0.264
AD Gem	3.787 980	0.164	–	1	0.219	0.159	0.144
DX Gem	3.137 486	0.507	–	1	0.462	–	0.430
Zeta Gem	10.150 135	0.031	0.041	11	0.044	0.033	0.009
V Lac	4.983 468	0.417	–	1	0.312	0.315	0.338
X Lac	5.444 990	0.350	–	1	0.330	0.339	0.336
Y Lac	4.323 776	0.136	0.011	9	0.226	0.202	0.195
Z Lac	10.885 613	0.415	0.043	9	0.375	0.378	0.368
RR Lac	6.416 243	0.363	–	1	0.284	0.296	0.353
BG Lac	5.331 932	0.272	0.020	3	0.358	0.316	0.287
V473 Lyr	1.490 780	0.091	–	1	0.049	–	–
T Mon	27.024 649	0.179	0.029	19	0.221	0.195	0.188
SV Mon	15.232 780	0.188	0.034	11	0.281	0.250	0.214
TW Mon	7.096 900	0.682	–	1	0.696	–	–
TX Mon	8.701 731	0.457	–	1	0.503	0.492	0.465
TZ Mon	7.428 014	0.448	–	1	0.462	0.431	–
UY Mon	2.397 970	0.163	–	1	0.108	–	–
WW Mon	4.662 310	0.688	–	1	0.602	0.561	–
XX Mon	5.456 473	0.610	–	1	0.623	0.586	–
AA Mon	3.938 164	0.724	–	1	0.814	0.791	–
AC Mon	8.014 250	0.579	–	1	0.750	0.702	0.776
EE Mon	4.808 960	0.509	–	1	0.539	0.507	–
CU Mon	4.707 873	0.859	–	1	0.792	0.750	–
CV Mon	5.378 898	0.681	–	1	0.488	0.464	–
EK Mon	3.957 941	0.518	–	1	0.582	0.551	–
FG Mon	4.496 590	0.625	–	1	0.684	0.650	–
FI Mon	3.287 822	0.607	–	1	0.539	0.513	–
V465 Mon	2.713 176	0.142	–	1	0.263	0.255	–
V504 Mon	2.774 050	0.588	–	1	0.565	–	–
V508 Mon	4.133 608	0.221	–	1	0.330	0.320	–
V526 Mon	2.674 985	0.218	–	1	0.093	–	–
S Nor	9.754 244	0.268	–	1	0.194	0.178	0.188
Y Oph	17.126 908	0.683	0.010	14	0.645	–	0.668
BF Oph	4.067 510	0.270	–	1	0.278	0.247	0.223
RS Ori	7.566 881	0.410	–	1	0.353	0.335	0.350
GQ Ori	8.616 068	0.272	–	1	0.238	0.228	0.268
SV Per	11.129 318	0.304	–	1	0.345	0.366	0.431
UX Per	4.565 815	0.522	–	1	0.492	0.512	–
VX Per	10.889 040	0.486	0.027	8	0.508	0.496	0.477
AS Per	4.972 516	0.685	–	1	0.728	0.644	0.685
AW Per	6.463 589	0.515	0.015	4	0.510	0.487	0.476
BM Per	22.951 900	0.975	0.016	4	0.978	0.870	–
HQ Per	8.637 930	0.543	–	1	0.571	–	–
MM Per	4.118 415	0.480	–	1	0.515	0.490	–
V440 Per	7.570 000	0.283	0.036	10	0.274	–	–
X Pup	25.961 000	0.429	0.033	7	0.421	0.409	0.399
RS Pup	41.387 600	0.515	–	1	0.480	0.453	0.480
VZ Pup	23.171 000	0.672	–	1	0.461	0.452	0.424
AD Pup	13.594 000	0.222	–	1	0.386	0.343	–

Table 2 – *continued*

Name	P (d)	$E(B-V)$	±	No. of spectra	$E(B-V)_{\rm Fer95}$	$E(B-V)_{\rm TSR03}$	$E(B-V)_{\rm LC07}$
AQ Pup	30.104 000	0.453	–	1	0.565	0.531	0.504
BN Pup	13.673 100	0.425	–	1	0.449	0.417	0.415
HW Pup	13.454 000	0.706	–	1	0.662	0.688	–
MY Pup	5.695 309	0.105	–	1	0.112	–	–
RV Sco	6.061 306	0.329	–	1	0.365	0.338	0.381
RY Sco	20.320 144	0.774	–	1	0.696	0.714	0.760
KQ Sco	28.689 600	0.893	–	1	0.906	0.839	0.911
V500 Sco	9.316 839	0.668:	0.158	9	0.603	0.568	0.621
Z Sct	12.901 325	0.560	–	1	0.569	0.491	0.534
S Sge	8.382 086	0.116	0.016	15	0.128	0.112	0.099
SS Sct	3.671 253	0.391	–	1	0.362	0.317	0.333
UZ Sct	14.744 200	0.986	–	1	1.020	0.973	–
EV Sct	3.090 990	0.737	–	1	0.663	–	0.650
U Sgr	6.745 229	0.398	0.022	9	0.434	0.403	0.421
W Sgr	7.594 904	0.079	0.017	8	0.116	0.112	0.108
X Sgr	7.012 877	0.219	–	2	0.201	0.201	0.230
Y Sgr	5.773 380	0.182	0.021	12	0.216	0.188	0.195
VY Sgr	13.557 200	1.136	–	1	0.961	1.143	–
WZ Sgr	21.849 789	0.458	0.058	12	0.486	0.428	0.467
XX Sgr	6.424 140	0.575	–	1	0.524	–	0.549
YZ Sgr	9.553 687	0.282	0.015	8	0.307	0.285	0.298
AP Sgr	5.057 916	0.186	–	1	0.196	0.174	0.195
AV Sgr	15.415 000	1.117	–	1	1.317	1.233	–
BB Sgr	6.637 102	0.287	–	1	0.303	0.276	0.315
V350 Sgr	5.154 178	0.280	–	1	0.328	0.295	0.330
ST Tau	4.034 299	0.306	0.076	3	0.349	0.339	0.393
SZ Tau	3.148 380	0.272	0.022	18	0.326	–	0.308
AE Tau	3.896 450	0.576	–	1	0.604	–	–
EF Tau	3.448 150	0.360	–	1	–	–	–
EU Tau	2.102 480	0.230	–	1	0.184	–	–
Alp UMi	3.969 600	−0.010	–	1	0.017	–	0.009
T Vel	4.639 819	0.272	–	1	0.300	0.271	0.286
RY Vel	28.135 700	0.602	–	1	0.573	0.554	0.540
RZ Vel	20.398 240	0.293	–	1	0.320	0.293	0.283
SW Vel	23.441 000	0.409	0.035	3	0.360	0.337	0.335
SX Vel	9.549 930	0.272	–	1	0.252	0.250	0.270
S Vul	68.464 000	0.940	0.051	6	0.782	0.737	0.674
T Vul	4.435 462	0.068	0.015	20	0.098	0.067	0.054
U Vul	7.990 629	0.663	0.018	7	0.636	0.593	0.640
X Vul	6.319 543	0.798	0.022	6	0.824	0.790	0.702
SV Vul	44.994 772	0.510	0.020	23	0.504	0.518	0.412

discrepant points in most cases represent Cepheids for which only single spectra are available. Here the problem is not of differences in reddening systems, but problems in the measurements for individual Cepheids.

All Cepheids undergo period changes (Turner et al. 2006a), some undergo random fluctuations in period (Berdnikov et al. 2004, 2007), and others display light traveltime effects from binarity and other curious changes to the times of light maximum (Turner et al. 2007) that affect the accurate determination of light-curve phasing, all of which are important factors for reddenings derived from spectroscopic and photometric observations. As noted previously, the problem is particularly acute for the present paper when only one spectrum has been obtained (see Turner, Usenko & Kovtyukh 2006b), which is the case for many of the Cepheids in the present sample. A number of objects in Table 2 are also suspected to be Type II Cepheids, but their [Fe/H] values are nearly solar according to the spectroscopic analyses.

Another comparison that can be made is with respect to colours derived from model atmospheres. Such a comparison is shown in Fig. 7, where the models (solid dots) are Kurucz (1992) models with the colours given by Castelli (1999). The models are for $\log g = 2.0$, $V_{\rm t} = 2.0\,{\rm km\,s^{-1}}$ and [Fe/H] = 0.0. The same parameters were used to generate intrinsic colours from the calibration determined here. As can be seen, the comparison is rather good. Over the larger part of the range the spectroscopic temperatures used here are 50–100 K lower than the temperatures that would be determined using the photometric calibration. Another way of stating this is that, at a fixed temperature, the theoretical photometric calibration would yield a $B-V$ colour excess about 0.05 mag smaller than found here. The difference between spectroscopic and photometric temperatures found here for high luminosity stars is in the same sense and magnitude as that found for spectroscopic versus photometric temperatures of dwarfs and giants (Luck & Heiter 2006, 2007).

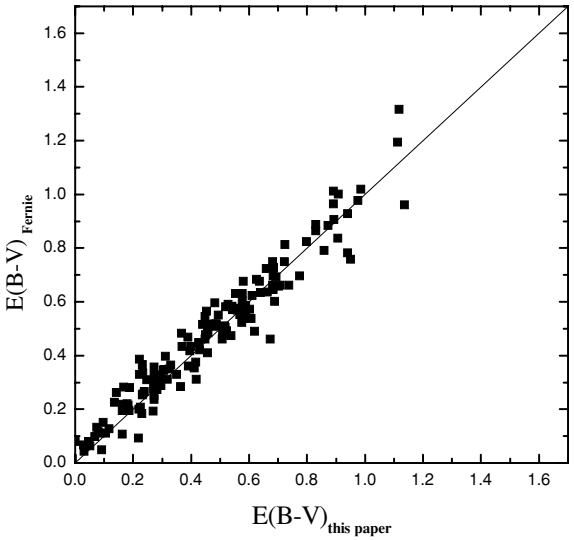

Figure 4. Comparison of our colour excesses with those of Fernie et al. (1995).

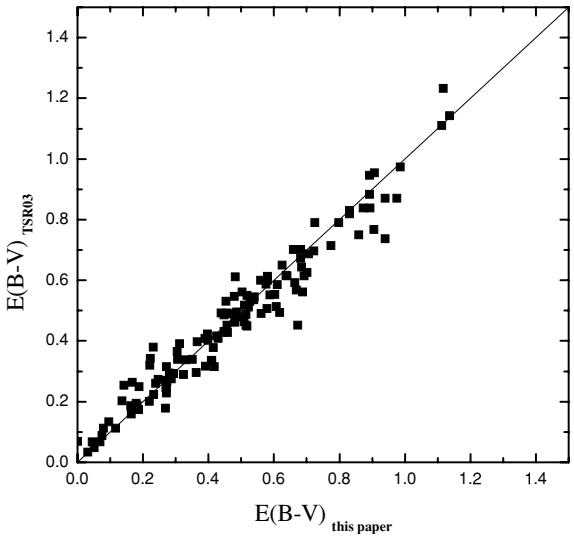

Figure 5. Comparison of the present colour excesses with those of Tammann et al. (2003).

It should be emphasized that high-resolution spectroscopic studies of Cepheids provide an independent source of reddenings that can be used to refine the existing reddening scale for Galactic Cepheids and to enhance the precision of the Cepheid PL relation. The colour excesses derived for Cepheids in our sample for which many spectra are available are quite likely more accurate than many previous estimates, and provide a good test of published reddening scales. Additional spectroscopic observations of Cepheids in our sample can only strengthen the present results, since they would eliminate the undersampling problem inherent to programme objects with $n = 1$. Correcting that deficiency should improve the precision of the overall sample.

6 SUMMARY

The present paper presents newly derived parameters, namely effective temperature ($T_{\rm eff}$), surface gravity ($\log g$), microturbulent velocity ($V_{\rm t}$, in km s^{-1}) and iron abundance ([Fe/H]), for 74 non-variable FGK supergiants, established from model atmosphere analyses of high-resolution spectra for the stars. Colour excesses have been computed for the stars on the basis of a new formulation of the relationship linking such parameters to intrinsic colour, $(B - V)_0$. The formulation has been extended to the 74 FGK supergiants and to a sample of 164 classical Cepheid variables to derive new estimates for their colour excesses $E(B - V)$, presented in Tables 1 and 2. The reddening estimates are demonstrated to be of extremely high internal precision, and to agree well with the most accurate estimates from the literature. The Cepheid reddenings, in particular, appear to be closely tied to the system of space reddenings that is presently available. Given the large distances of supergiants, the method opens the possibility for large-scale extinction mapping of the Galaxy, with a sensitivity of 0.08–0.2 mag.

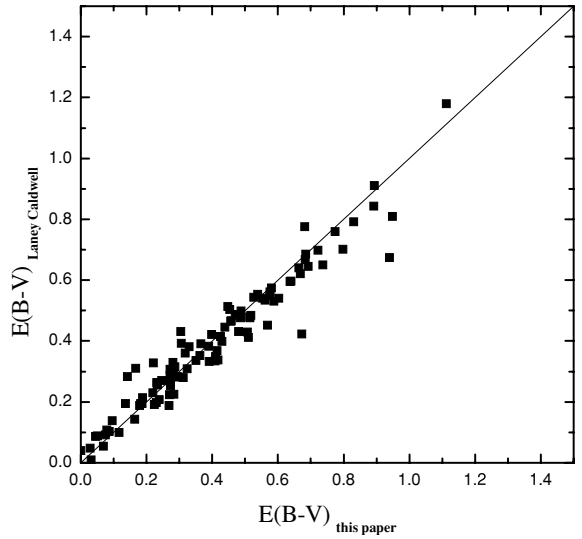

Figure 6. Comparison of the present colour excesses with those of Laney & Caldwell (2007).

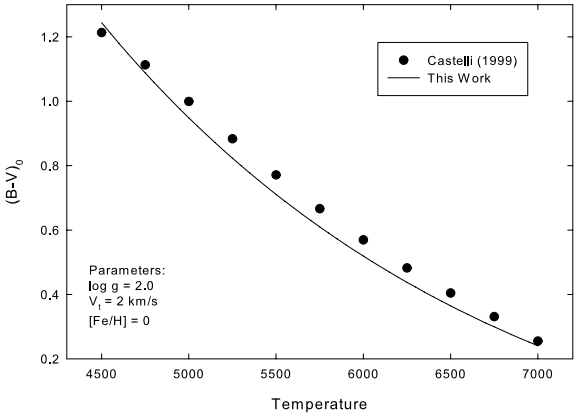

Figure 7. Comparison of the present colours with those of Castelli (1999).

ACKNOWLEDGMENTS

This work is based on spectra collected with the 1.93-m telescope of the OHP (France) and the ESO Telescopes at the Paranal Observatory under programme ID266.D-5655. We thank the referee for useful suggestions that helped to improve the presentation.

REFERENCES

Andrievsky S. M. et al., 2002a, A&A, 381, 32
Andrievsky S. M., Bersier D., Kovtyukh V. V., Luck R. E., Maciel W. J., Lepine J. R. D., Beletsky Yu. V., 2002b, A&A, 384, 140
Andrievsky S. M., Kovtyukh V. V., Luck R. E., Lepine J. R. D., Maciel W. J., Beletsky Yu. V., 2002c, A&A, 392, 491
Andrievsky S. M., Luck R. E., Kovtyukh V. V., 2005, AJ, 130, 1880
Bagnulo S. et al., 2003, ESO Messenger, 114, 10
Baranne A. et al., 1996, A&AS, 119, 373
Berdnikov L. N., 2007, http://www.sai.msu.ru/groups/cluster/CEP/PHE
Berdnikov L. N., Samus N. N., Antipin S. V., Ezhkova O. V., Pastukhova E. N., Turner D. G., 2004, PASP, 116, 536
Berdnikov L. N., Pastukhova E. N., Gorynya N. A., Zharova A. V., Turner D. G., 2007, PASP, 119, 82
Bersier D., 1996, A&A, 308, 514
Castelli F., 1999, A&A, 346, 564
Feltz K. A. Jr, 1972, PASP, 84, 497
Fernie J. D., 1987, AJ, 94, 1003
Fernie J. D., Evans N. R., Beattie B., Seager S., 1995, Inf. Bull. Variable Stars, 4148
Fry A. M., Carney B. W., 1999, AJ, 118, 1806
Galazutdinov G. A., 1992, preprint Special Astrophysical Observatory of Russian Academy of Science 92, 28
Gray D. F., 1992, The Observation and Analysis of Stellar Photospheres. Cambridge Univ. Press, Cambridge
Katz D., Soubiran C., Cayrel R., Adda M., Cautain R., 1998, A&A, 338, 151
Kovtyukh V. V., 2007, MNRAS, 378, 617
Kovtyukh V. V., Andrievsky S. M., 1999, A&A, 351, 597
Kovtyukh V. V., Andrievsky S. M., Belik S. I., Luck R. E., 2005, AJ, 129, 433
Kraft R. P., 1960, ApJ, 131, 330
Kurucz R. L., 1992, in Barbuy B., Renzini A., eds, IAU Symp. 149, The Stellar Population of Galaxies. Kluwer, Dordrecht, p. 225
Laney C. D., Caldwell J. A. R., 2007, MNRAS, 377, 147
Luck R. E., Heiter U., 2006, AJ, 131, 3069
Luck R. E., Heiter U., 2007, AJ, 133, 2464
Luck R. E., Gieren W., Andrievsky S. M., Kovtyukh V. V., Fouqué P., Pont F., Kienzle F., 2003, A&A, 401, 939
Luck R. E., Kovtyukh V. V., Andrievsky S. M., 2006, AJ, 132, 902
McNamara D. H., Potter D., 1969, PASP, 81, 545
McNamara D. H., Helm T. M., Wilcken S. K., 1970, PASP, 82, 293
Moultaka J., Ilovaisky S. A., Prugniel P., Soubiran C., 2004, PASP, 116, 693
Pel J. W., Lub J., 1978, in Philip A. G. D., Hayes D. S., eds, IAU Symp. 80, The HR Diagram: The 100th Anniversary of Henry Norris Russell. Reidel, Dordrecht, p. 229
Sasselov D. D., Lester J. B., 1990, ApJ, 360, 227
Schmidt E. G., Taylor D. J., 1979, AJ, 84, 1192
Spencer Jones J. H., 1989, MNRAS, 238, 269
Tammann G. A., Sandage A., Reindl B., 2003, A&A 404, 423
Turner D. G., 1995, in Stobie R. S., Whitelock P. A., eds, IAU Colloq. 155, ASP Conf. Ser. Vol. 83, Astrophysical Applications of Stellar Pulsation. Astron. Soc. Pac., San Francisco, p. 256
Turner D. G., 2001, Odessa Astron. Publ., 14, 166
Turner D. G., Burke J. F., 2002, AJ, 124, 2931
Turner D. G., Leonard P. J. T., English D. A., 1987, AJ, 93, 368
Turner D. G., Abdel-Sabour Abdel-Latif M., Berdnikov L. N., 2006a, PASP, 118, 410
Turner D. G., Usenko I. A., Kovtyukh V. V., 2006b, Observatory, 126, 207
Turner D. G. et al., 2007, PASP, 119, 1247
Turner D. G., MacLellan R. F., Henden A. A., Berdnikov L. N., 2008, PASP, submitted

This paper has been typeset from a TEX/LATEX file prepared by the author.